Biophysical Chemistry 145 (2009) 86–90

Contents lists available at ScienceDirect

Biophysical Chemistry

journal homepage: http://www.elsevier.com/locate/biophyschem

Potential of mean force of the hepatitis C virus core protein–monoclonal 19D9D6 antibody interaction

Yeng-Tseng Wang [a,b,*], Zhi-Yuan Su [c], Cheng-Lung Chen [b,*]

[a] National Center for High-performance Computing, Hsin-Shi, Tainan County, Taiwan
[b] The Department of Chemistry, National Sun Yat-Sen University, Kaohsiung 804, Taiwan
[c] The Department of Information Management, Chia Nan University of Pharmacy and Science, Tainan 717, Taiwan

ARTICLE INFO

Article history:
Received 17 June 2009
Received in revised form 4 August 2009
Accepted 12 September 2009
Available online 22 September 2009

Keywords:
Molecular dynamics
Potential of mean force
Hepatitis C virus
Antibody

ABSTRACT

Antigen–antibody interactions are critical for understanding antigen–antibody associations in immunology. To shed further light on this question, we studied a dissociation of the 19D9D6-HCV core protein antibody complex structure. However, forced separations in single molecule experiments are difficult, and therefore molecular simulation techniques were applied in our study. The stretching, that is, the distance between the center of mass of the HCV core protein and the 19D9D6 antibody, has been studied using the potential of mean force calculations based on molecular dynamics and the explicit water model. Our simulations indicate that the 7 residues Gly70, Gly72, Gly134, Gly158, Glu219, Gln221 and Tyr314, the interaction region (antibody), and the 14 interprotein molecular hydrogen bonds might play important roles in the antigen–antibody interaction, and this finding may be useful for protein engineering of this antigen–antibody structure. In addition, the 3 residues Gly134, Gly158 and Tyr314 might be more important in the development of bioactive antibody analogs.

1. Introduction

Stretching mechanics is an important factor for understanding antigen–antibody associations and improving antigen–antibody binding efficiency in immunology. The hepatitis C virus (HCV) is a small enveloped RNA virus, which causes human acute hepatitis and chronic liver disease [1]. Globally, an estimated 170 million people, i.e. 3% of the world's population, are chronically infected with HCV, and 3–4 million people are newly infected each year. The HCV genome consists of a single-stranded, positive-sense RNA of 9.6 kb that encodes a polyprotein of approximately 3000 amino acids [2]. The HCV polyprotein is processed by host cellular and viral proteases to yield at least 10 structural and nonstructural (NS) proteins, including core protein, envelope glycoproteins (E1 and E2), p7, NS2, NS3, NS4A, NS4B, NS5A and NS5B [3,4]. The core protein (119 amino acids) is a highly basic RNA-binding protein that presumably forms the viral nucleocapsid. The core antigen peptide (Ag) is highly conserved among the various HCV genotypes [5] and elicits a rapid antibody response after the onset of the disease. Thus, the core Ag is an important target for the induction of antiviral immune responses [1]. Stura [6] used X-ray crystallography and identified the interaction region on the antibodies (Thr250, Asp251, Phe252, Ser253, Trp270, Val271, Thr272, Asn273, Glu274, Gln323, Asn31, Arg33, Thr34, Tyr38, His41, Trp56, Ala97, Tyr98, Pro100, Leu102, Leu103 and Gln105) and 14 intermolecular hydrogen bonds (Table 1) that may play important roles in binding the 19D9D6 antibody. However, it is difficult to study antigen–antibody binding mechanics by using experimental instruments, and thus molecular dynamics (MD) simulations have been more readily applied to analyze complex structure binding mechanics.

The potential of mean force (PMF) method is a practical method that enables better understanding of the binding interactions between 2 groups of molecules. With regard to biological systems such as protein–ligand [7–9] and protein–protein systems [10], the PMF can be used to analyze the intermolecular interactions. The PMF for stretching the complex structure for equilibrium MD simulations was calculated using umbrella sampling techniques and the weighted histogram analysis method (WHAM). Computations on the stretching of the complex structure were performed using a TIP3P solvent model [11]. The stretching distance ranged from 3.5 to 5.5 nm.

The cumulative changes in dihedral angles (CCDAs) method is useful to predict important residues in the biomolecule dissociation systems [10,12]. In the biomolecule systems, backbone rotations are provided with higher energy barriers, [13–16] and backbone dihedral angles are representative of backbone rotations. Thus, we consider that the counting of the cumulative changes in backbone dihedral angles from the trajectories determined using the biomolecule dissociation systems is useful in predicting important residues.

Previous studies have used binding hot spots methods to predict important key residues in protein–protein interactions from known 3D structures or protein sequences [17–19]. The KFC method has been successfully applied to predict the hot spots in protein–protein interactions, such as calmodulin-smooth muscle myosin light chain

* Corresponding authors. Fax: +886 5050940, +886 7 5252630.
E-mail addresses: c00jsw00@nchc.org.tw (Y.-T. Wang), chen1@mail.nsysu.edu.tw (C.-L. Chen).

0301-4622/$ – see front matter © 2009 Elsevier B.V. All rights reserved.
doi:10.1016/j.bpc.2009.09.004

Table 1
The 14 intermolecular hydrogen bonds.

The number of hydrogen bonds	Hepatitis C virus core protein atom	Monoclonal 19D9D6 antibody atom
Hepatitis C virus core protein interactions with heavy chain antibody		
1	Gln443 O	Ser253 N
2	Gln443 O	Thr272 N
3	Gln443 N	Thr272 O
4	Gln443 N	Glu274 N
5	Gly446 N	Gln323 O
6	Val448 O	Ser411 O
7	Tyr449 O	Ser359 O
Hepatitis C virus core protein interactions with light chain antibody		
8	Gly447 N	Ala97 O
9	Gly447 N	Tyr98 O
10	Gly447 O	Asn31 N
11	Val448 N	Tyr98 O
12	Leu450 O	Asn31 N
13	Arg453 NH1	Ssr7 O
14	Arg453 NH2	Ser7 O

kinase interface and the bone morphogenetic protein (BMP)-receptor interface [17]. Results from the KFC method indicate a strong correlation between KFC hot spot predictions and mutations that significantly reduce the binding affinity of the interface. Therefore, the KCF method was applied to compare the results of our stretching process.

In the present study, MD simulations were performed to evaluate the stretching of the HCV Ag–antibody complex structure. Detailed analysis of the MD simulations revealed the PMF, profile of CCDAs, the pair interactions of the interaction region (antibody)–HCV core protein, the root mean square displacement (RMSD) of the interaction region (antibody), and the distance trajectories of the 10 hydrogen bonds (DTOHB) in the stretching process.

2. Methods

2.1. Initial model systems of the HCV Ag–antibody complex

In previous studies, several HCV Ag–antibody complex structures were resolved and deposited in protein data banks [6,20]. We used the X-ray structure of the HCV Ag monoclonal 19D9D6 antibody (PDB ID: 1 N64) as our initial model, because the interactions of these complex structures have been well studied by Stura [6]. This model was assigned protonation states at pH 6.5 [21,22] as shown in Fig. 1.

2.2. Computational models and details

Calculations were performed with the software program CHARMM [23] using the CHARMM parameters (par_all27_prot_na) and the TIP3P solvent model. All MD simulations were performed in the canonical ensemble [24] (the simulation temperature was 310 K), unless stated otherwise, using the Verlet integrator with an integration time step of 0.002 ps and SHAKE [25] of all covalent bonds involving hydrogen atoms. In electrostatic interactions, atom-based truncation was performed using the particle-mesh Ewald (PME) [26] method, and the switch van der Waals function was used with a 1.8-nm cutoff for atom-pair lists. The complex structure was minimized for 10,000 conjugate gradient steps, and was then subjected to a 1-ns isothermal, constant volume MD simulation. The final structure was used to initiate PMF calculations, and the MD trajectories were used to calculate the normal CCDA and KFC hot spots.

2.3. PMF calculations (Helmholtz free energy)

The CHARMM miscellaneous mean field potential (MMFP) was applied to the stretching constraints, i.e. the distance constraints

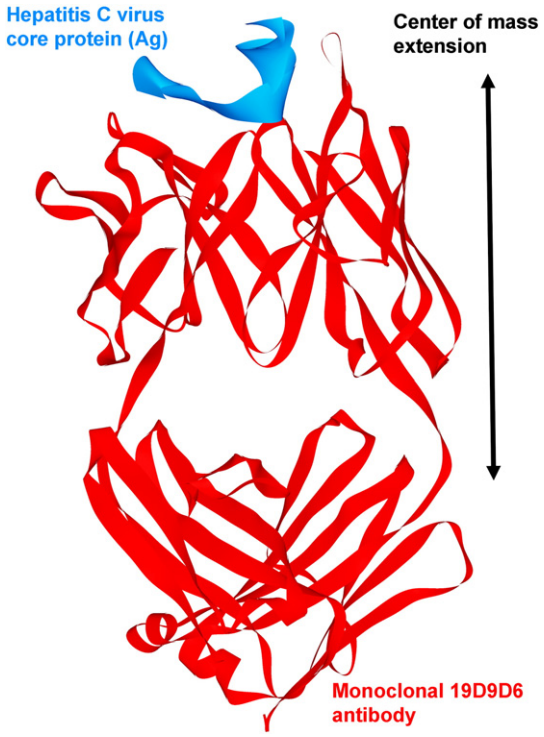

Fig. 1. Model for the stretching (center of mass extension) simulation on the 19D9D6 antibody–HCV core protein antibody complex.

between the center of mass of the HCV core protein and the 19D9D6 antibody with a force constant of 10.0 kcal/mol. The PMF calculations used a reaction coordinate (r), defined as the distance between the center of mass of the HCV core Ag protein and the monoclonal 19D9D6 antibody, to describe the complex structure binding mechanics. The r value varied from 3.5 to 5.5 nm in 0.05-nm increments. The MD simulations for PMF determination were performed with an initial 0.5-ns equilibration followed by 1-ns sampling at a given r value.

The WHAM [27] method was used to analyze molecular dynamics or Monte Carlo simulation data. WHAM minimizes the error in the density-of-states function (Ω) and facilitates the calculation of free energy surfaces. In each simulation, 2 quantities were monitored: the total system potential energy (V) and the total numbers of r (N_{NL}). Calculating Ω for 2 quantities is computationally impractical; therefore, it was necessary to calculate several Ω values, each a function of different thermodynamic parameters. The formula for Ω is

$$\Omega(V, N_{NL}) = \frac{\sum_{j=1}^{k} N_k(V, N_{NL})}{\sum_{j=1}^{k} n_j \exp(-f_j - \beta_j V)} \quad (1)$$

where N_{NL} and V are the monitored parameters; N_k is the number of occurrences for sampling with (V, N_{NL}); f_j is equal to βA_j, where A_j is the free energy of simulation j; β is $1/k_BT$; k is the number of simulations; and n_j is the number of samples from simulation j. The free energies were calculated by solving

$$P_\beta(V, N_{NL}) = \frac{\sum_{i=1}^{k} N_i(V, N_{NL}) \exp(-\beta V)}{\sum_{j=1}^{k} n_j \exp(-f_j - \beta_j V)} \quad (2)$$

$$\exp(-f_k) = \sum_{V, N_{NL}} P_{\beta_k}(V, N_{NL}) \quad (3)$$

where P_β is the probability of observing a sample with (V,N_{NL}). Thermodynamic averages were calculated from

$$<N_{NL}> = \frac{\sum_{V,N_{NL}}(N_{NL})^*\Omega(V,N_{NL})\exp(-\beta V)}{\sum_{V,N_{NL}}\Omega(V,N_{NL})\exp(-\beta V)} \quad (4)$$

using N_{NL} as an example. Free energies were calculated as follows:

$$F(N_{NL}) = -k_B T \ln\{P_\beta(N_{NL})\} \quad (5)$$

$$P_\beta(N_{NL}) = \sum_V P_\beta(V,N_{NL}) \quad (6)$$

Rosta et al. [28] recently highlighted improvements in the WHAM method, and using their approach, it was easy to avoid possible artifacts in estimating barriers and free energy profiles on a 1-D projection in a systematic way.

3. Results and discussion

3.1. PMF profile, DTOHB, normal range of CCDA, and KFC hot spots

The PMF profile is shown in Fig. 2A, and the PMF change was found to be 55.81 kcal/mol in the stretching process. The distance trajectories of the 14 intermolecular hydrogen bonds are shown in Fig. 2B, and the hydrogen bonds (8th, 9th, 10th and 11th) appear to play important roles in the stretching process.

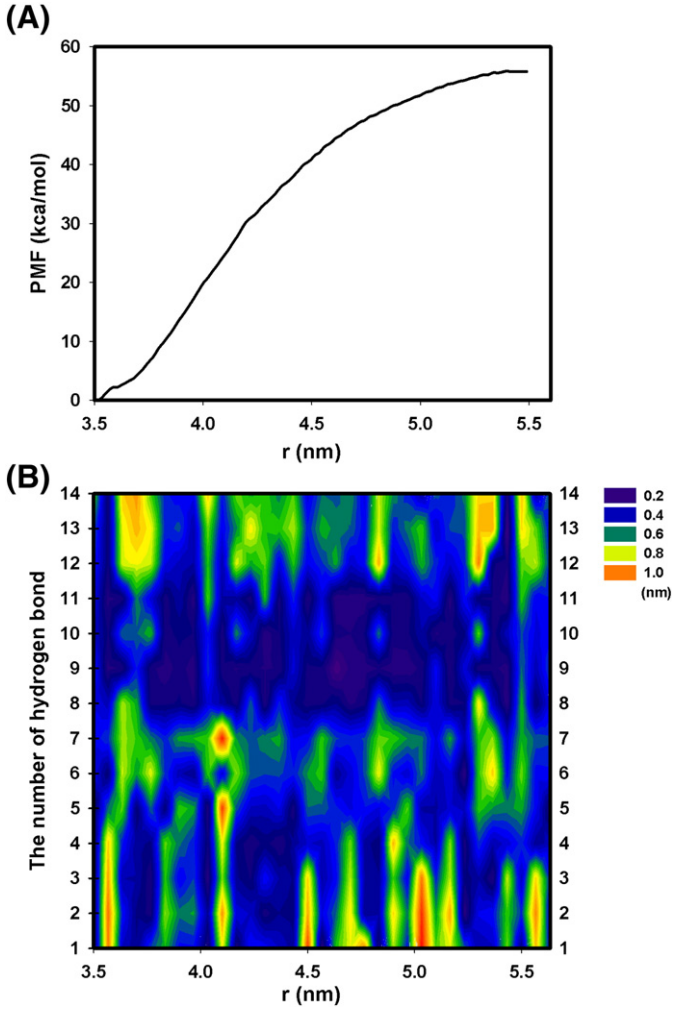

Fig. 2. (A) The calculated PMF profile (r, 3.5–5.5 nm). (B) The distance trajectories of the 14 intermolecular hydrogen bonds.

The normal range of CCDA is shown in Table 2. The average of all the amino acid CCDAs was less than 30°, and the maximum CCDA was less than 300°. From these results, it appears that a large CCDA (more than 300°) is important in complex binding mechanics. The stretching CCDAs are shown in Fig. 3, and there are obvious variations in the phi or psi angles of the residues Gly70, Gly72, Gly134, Gly158, Gln221, Tyr314, Pro439, Gly440, Gly441, Gly442, Gln443 and Gly446.

The KFC hot spots are shown in Fig. 4. The results indicate that the residues Tyr32, Try36, Trp50, Leu96, Phe98, Gly134, Gly158, Ser176, Phe309, Arg312, Tyr314, Trp317 and Phe380 of the antibody are important key residues in the antigen–antibody interaction.

3.2. The RMSD and pair interactions of the interaction region (antibody)

The RMSD of the interaction region is shown in Fig. 5A, and the value was less than 2.5 during the stretching process. The pair interactions between the interaction region and the HCV core protein are shown in Fig. 5B. When the reaction coordinate r was less than 4.5 nm, the pair interactions were strong, especially when the r value was 3.5 nm (equal to −210.08 kcal/mol). The pair interactions rapidly diminished between the r values of 4.3 and 4.5 nm, and when the r value was greater than 4.5 nm, the pair interactions were equal to 0.

3.3. Analysis of the monoclonal 19D9D6 antibody–HCV core protein stretching process

The stretching CCDA of the monoclonal 19D9D6 antibody were individually traced in the 3 major regions on the basis of the pair interactions between the interaction region and the HCV core protein (r of 3.5–4.3 nm, 4.3–4.5 nm and 4.5–5.5 nm). These results are shown in Table 3. In the first region, the 3 residues Gly70, Gly72, and Thr314 and the 14 hydrogen bonds (DTOHB was less than 0.5 nm) all played an important role and improved antigen–antibody complex formation. The RMSD and the pair interactions (the interaction region) of each of these residues were less than 2.14 and −58.74 kcal/mol, respectively. In the second region, the 3 residues Gly70, Gly72 and Thr314 had strongly rotated dihedral angles. The RMSD and the pair interactions (the

Table 2
The normal range of the CCDA of the amino residues (the monoclonal 19D9D6 antibody–HCV core protein complex structure).

Amino residue	Cumulative changes in the dihedral angles (°)			
	Maximum phi (Φ)	Maximum psi (Ψ)	Average phi (Φ)	Average psi (Ψ)
Ala	92.00	136.00	14.00	16.00
Arg	106.00	90.00	22.00	16.00
Asn	93.00	254.00	14.00	19.00
Asp	100.00	149.00	13.00	23.00
Cys	74.00	143.00	13.00	23.00
Gln	97.00	196.00	17.00	14.00
Glu	108.00	100.00	19.00	15.00
Gly	231.00	297.00	20.00	20.00
Hse	96.00	86.00	14.00	14.00
Ile	73.00	44.00	11.00	9.00
Leu	114.00	62.00	16.00	12.00
Lys	298.00	69.00	16.00	11.00
Met	52.00	97.00	13.00	14.00
Phe	73.00	55.00	12.00	11.00
Pro	67.00	112.00	16.00	15.00
Ser	110.00	93.00	18.00	14.00
Trp	93.00	63.00	13.00	13.00
Tyr	57.00	162.00	12.00	11.00
Val	54.00	25.00	13.00	11.00

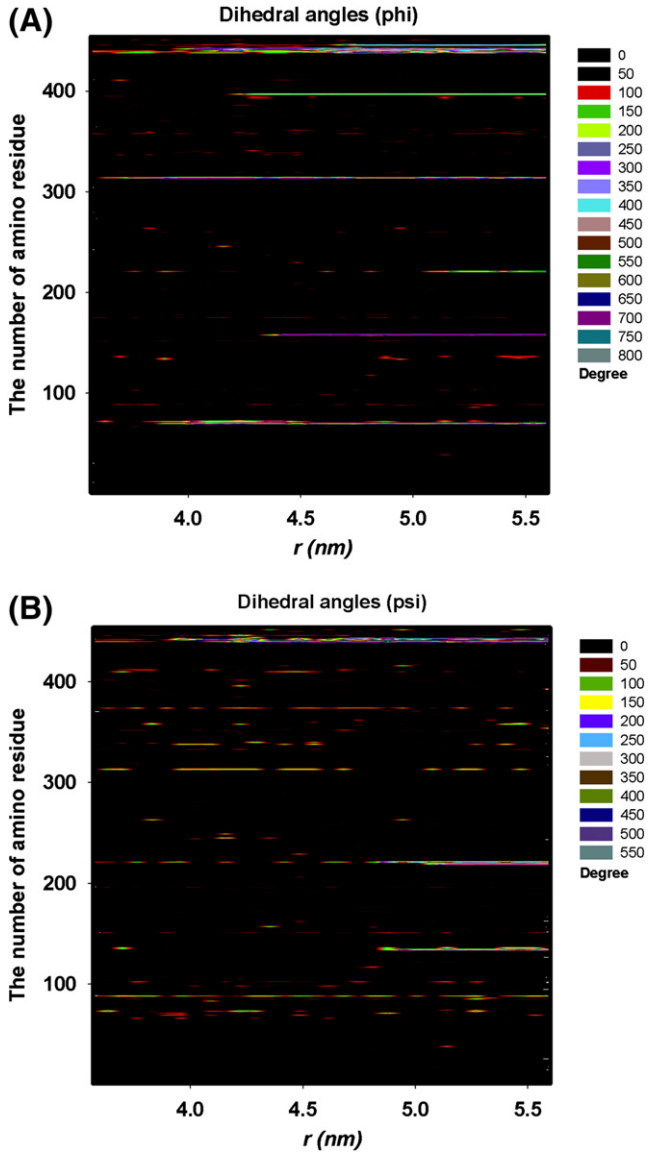

Fig. 3. A profile of the cumulative changed dihedral angles (phi and psi) for the values of *r* ranging from 3.5 to 5.5 nm. Here, the amount of residues ranges from 1 to 438 (the 19D9D6 antibody) and 439 to 454 (the HCV core protein).

Fig. 4. Binding hot spots prediction (KFC method) for the 19D9D6 antibody–HCV core protein antibody complex. The small green particles present indicate the binding hot spots in the complex. (For interpretation of the references to color in this figure legend, the reader is referred to the web version of this article.)

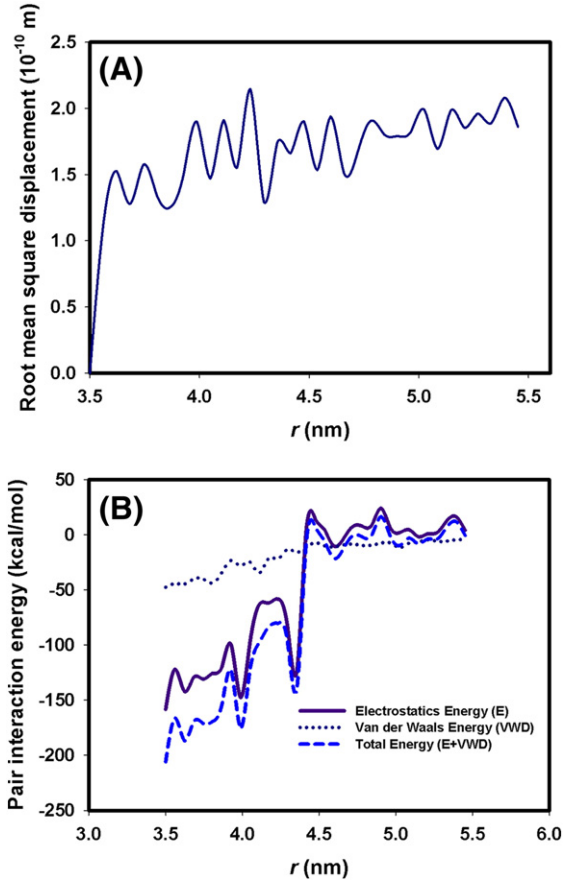

Fig. 5. (A) RMSD of the interaction region (antibody). (B) Pair interaction of the interaction region (antibody).

interaction region) of these residues ranged between 1.29 and 1.74 kcal/mol and between −140.82 and 21.15 kcal/mol, respectively. In the third region, the 6 residues Gly72, Gly134, Gly158, Glu219, Gln221 and Tyr314 had dihedral angles that were rotated more than 300°. The RMSD and the pair interactions (the interaction region) of these residues ranged from 1.51 to 1.86 kcal/mol and from −21.05 to 24.15 kcal/mol.

Our simulation results suggest that there are 3 major regions in the complex structure binding mechanics, and that the interaction region and the 7 residues Gly70, Gly72, Gly134, Gly158, Glu219, Gln221 and Tyr314 play a significant role in relaxing the complex structure, thus making it relatively easy to bind together. At an *r* value of 3.5–4.3 nm, the interaction region and the 14 hydrogen bonds might improve the ease by which the complex structure overcomes the first energy barriers. The comparison of our simulation results with the KFC hot spots revealed 3 common important key residues Gly134, Gly158 and Tyr314. The 3 residues may play a more important role in the antigen–antibody interaction.

Table 3
The amino residues of the monoclonal 19D9D6 antibody for which the CCDA is more than 300° when *r* value ranges from 3.5 to 4.3, 4.3 to 4.5 and 4.5 to 5.5.

r (nm)	The no. of amino residue	Cumulative changes in dihedral angles (°)	
		Phi (Φ)	Psi (Ψ)
3.5–4.3	Gly70	376.00	7.00
	Gly72	346.00	5.00
	Tyr314	358.00	4.00
4.3–4.5	Gly70	384.00	19.00
	Gly158	360.00	5.00
	Tyr314	524.00	64.00
4.5–5.5	Gly70	547.00	26.00
	Gly134	31.00	372.00
	Gly158	365.00	8.00
	Glu219	0.00	355.00
	Gln221	315.00	317.00
	Tyr314	365.00	4.00

4. Conclusions

In this study, we proposed the stretching of the 19D9D6 antibody–HCV core protein complex structure to predict the binding mechanics and the free energy profile, and carried out the stretching of the 19D9D6 antibody–HCV core protein complex with MD simulations. We used the WHAM method to extract the PMF profile from the MD simulations, and found that 3 major regions are involved in the stretching process. In addition, we used CCDAs, RMSD/pair interactions of the interaction region (antibody), and fourteen intermolecular hydrogen bonds to analyze these 3 regions. The comparison of our simulation results with the KFC hot spots revealed 3 common residues (Gly134, Gly158, and Tyr314). These results suggest that the 7 residues Gly70, Gly72, Gly134, Gly158, Glu219, Gln221 and Tyr314, the interaction region (antibody) and the 14 interprotein molecular hydrogen bonds might play an important role in the antigen–antibody interaction. In addition, the 3 residues Gly134, Gly158 and Tyr314 might be more important in the development of bioactive antibody analogs. We plan to verify our simulation results by conducting further molecular biology experiments.

Acknowledgments

This work was supported by the National Center for High-Performance Computing and the National Sun Yat-Sen University, Taiwan.

References

[1] H.J. Park, S.M. Byun, Y.J. Ha, J.S. Ahn, H.M. Moo, Identification of immunodominant epitopes in the core and non-structural region of hepatitis C virus by enzyme immunoassay using synthetic peptides, J. Immunoassay 16 (1995) 167–181.
[2] Q.L. Choo, G. Kuo, A.J. Weiner, L.R. Overby, L.R. Bradley, M. Houghton, Isolation of a cDNA clone derived from a blood-borne non-A, non-B viral hepatitis genome, Science 244 (1989) 359–362.
[3] B.D. Lindenbach, C.M. Rice, Unraveling hepatitis C virus replication from genome to function, Nature 436 (2005) 933–938.
[4] N. Appel, T. Schaller, F. Penin, R. Bartenschlager, From structure to function: new insights into hepatitis C virus RNA replication, J. Biol. Chem. 281 (2006) 9833–9836.
[5] M. Houghton, A. Weiner, J. Han, G. Kuo, Q.L. Choo, Molecular biology of the hepatitis C virus: implications for diagnosis, development, and control of viral disease, Hepatology 14 (1991) 381–388.
[6] R. Me´nez, M. Bossus, B.H. Muller, G. Sibaı, P. Dalbon, F. Ducancel, C. Jolivet-Reynaud, E.A. Stura, Crystal structure of a hydrophobic immunodominant antigenic site on hepatitis C virus core protein complexed to monoclonal antibody 19D9D61, J. Immunol. 170 (2003) 1917–1924.
[7] T. Batuğ, P.C. Chen, S.M. Patra, S. Kuyucak, Potential of mean force calculations of ligand binding to ion channels from Jarzynski's equality and umbrella sampling, J. Chem. Phys. 128 (2008) 155104–155114.
[8] M.S. Lee, M.A. Ison, Calculation of absolute protein–ligand binding affinity using path and endpoint approaches, Biophys. J. 19 (2006) 864–877.
[9] H.J. Woo, B. Roux, Calculation of absolute protein–ligand binding free energy from computer simulations, Proc. Natl. Acad. Sci. 19 (2005) 6825–6830.
[10] Y.T. Wang, J.M. Liaob, C.L. Chen, Z.Y. Su, C.H. Chen, J.J. Hu, Potential of mean force for human lysozyme–camelid vhh hl6 antibody interaction studies, Chem. Phys. Lett. 455 (2008) 284–288.
[11] H.J.C. Berendsen, J.R. Grigera, T.P. Straatsma, Molecular dynamics with coupling to an external bath, J. Phys. Chem. 91 (1987) 6269–6271.
[12] Y.T. Wang, Z.Y. Su, J.M. Liao, C.L. Chen, Potential of mean force for Syrian hamster prion epitope protein–Monoclonal fab 3f4 antibody interaction studies, Eur. J. Med. Chem. 44 (2009) 3504–3508.
[13] C.A. Smith, T. Kortemme, Backrub-like backbone simulation recapitulates natural protein conformational variability and improves mutant side-chain prediction, J. Mol. Biol. 380 (2008) 742–756.
[14] G.D. Henry, J.H. Weiner, B.D. Sykes, Backbone dynamics of a model membrane protein: 13C NMR spectroscopy of alanine methyl groups in detergent solubilized M13 coat protein, Biochem. 25 (1986) 590–598.
[15] J.P. Ulmschneider, W.L. Jorgensen, Monte Carlo backbone sampling for polypeptides with variable bond angles and dihedral angles using concerted rotations and a Gaussian bias, J. Chem. Phys. 118 (2003) 4261–4271.
[16] K. Gunasekaran, L. Gomathi, C. Ramakrishnan, J. Chandrasekhar, P. Balaram, Conformational interconversions in peptide beta-turns: analysis of turns in proteins and computational estimates of barriers, J. Mol. Biol. 284 (1998) 1505–1516.
[17] S.J. Darnell, D. Page, J.C. Mitchell1, An automated decision-tree approach to predicting protein interaction hot spots, Proteins 68 (2007) 813–823.
[18] Y. Ofran1, B. Rost1, Protein–protein interaction hotspots carved into sequences, PLoS. Comput. Biol. 3 (2007) 1169–1176.
[19] N. Tuncbag, A. Gursoy, O. Keskin, Identification of computational hot spots in protein interfaces, Bioinformatics 25 (2009) 1513–1520.
[20] R. Menez, N.G. Housden, S. Harrison, C. Jolivet-Reynaud, M.G. Gore, E.A. Stura, Different crystal packing in Fab-protein L semi-disordered peptide complex, Acta Crystallogr. 61 (2005) 744–749.
[21] J.C. Gordon, J.B. Myers, T. Folta, V. Shoja, L.S. Heath, A. Onufriev, H++: a server for estimating pKas and adding missing hydrogens to macromolecules, Nucleic Acids Res. 33 (2005) W368–71.
[22] R. Anandakrishnan, A. Onufriev, Analysis of basic clustering algorithms for numerical estimation of statistical averages in biomolecules, J. Comp. Biol. 15 (2008) 165–184.
[23] B.R. Brooks, R.E. Bruccoleri, B.D. Olafson, D.J. States, S. Swaminathan, M. Karplus, CHARMM: a program for macromolecular energy, minimization, and dynamics calculations, J. Comp. Chem. 4 (1983) 187–217.
[24] J.P. Ryckaert, G. Ciccotti, Andersen's canonical-ensemble molecular dynamics for molecules with constraints, Mol. Phys. 58 (1986) 1125–1136.
[25] J.P. Ryckaert, G. Ciccotti, H.J.C. Berendsen, Numerical integration of the Cartesian equations of motion of a system with constraints: molecular dynamics of n-alkanes, J. Comp. Phys. 23 (1977) 327–341.
[26] T. Darden, D. York, L. Pederson, Particle-mesh Ewald: an N log(N) method for Ewald sums in large systems, J. Chem. Phys. 98 (1993) 10089–10092.
[27] S. Kumar, D. Bouzida, R.H. Swendsen, P.A. Kollman, J.M. Rosenberg, The weighted histogram analysis method for free-energy calculations on biomolecules. I. The method, J. Comp. Chem. 13 (1992) 1011–1021.
[28] E. Rosta, H.L. Woodcock, B.R. Brooks, G. Hummer, Artificial reaction coordinate, "tunneling" in free-energy calculations: the catalytic reaction of RNase H, J. Comp. Chem. 30 (2009) 1634–1641.